Eurasian Journal of Physics and Functional Materials

Volume 4 | Number 1

Article 8

Pages: 67 - 85

3-22-2020

Phase composition and thermoelectric properties of the nanocomposite alloys NaxCu2-x-yS

M. M. Kubenova
L.N. Gumilyov Eurasian National University ,Kazakhstan

M. Kh. Balapanov
Bashkir State University ,Russian Federation

K. A. Kuterbekov
L.N. Gumilyov Eurasian National University ,Kazakhstan

R. Kh. Ishembetov
Bashkir State University ,Russian Federation

A. M. Kabyshev
L.N. Gumilyov Eurasian National University ,Kazakhstan

See next page for additional authors

Follow this and additional works at: https://www.ephys.kz/journal

 Part of the Materials Science and Engineering Commons, and the Physics Commons

Recommended Citation

Kubenova, M. M.; Balapanov, M. Kh.; Kuterbekov, K. A.; Ishembetov, R. Kh.; Kabyshev, A. M.; and Yulaeva, Y. Kh. (2020) "Phase composition and thermoelectric properties of the nanocomposite alloys NaxCu2-x-yS," *Eurasian Journal of Physics and Functional Materials*: Vol. 4: No. 1, Article 8.
DOI: https://doi.org/10.29317/ejpfm.2020040108

This Original Study is brought to you for free and open access by Eurasian Journal of Physics and Functional Materials. It has been accepted for inclusion in Eurasian Journal of Physics and Functional Materials by an authorized editor of Eurasian Journal of Physics and Functional Materials.

Phase composition and thermoelectric properties of the nanocomposite alloys NaxCu2-x-yS

Authors

M. M. Kubenova, M. Kh. Balapanov, K. A. Kuterbekov, R. Kh. Ishembetov, A. M. Kabyshev, and Y. Kh. Yulaeva

This original study is available in Eurasian Journal of Physics and Functional Materials: https://www.ephys.kz/journal/vol4/iss1/8

Eurasian Journal of Physics and Functional Materials

2020, 4(1), 67-85

Phase composition and thermoelectric properties of the nanocomposite alloys $Na_xCu_{2-x-y}S$

M.M. Kubenova*,[1], M.Kh. Balapanov[2], K.A. Kuterbekov[1], R.Kh. Ishembetov[2], A.M. Kabyshev[1], Y.Kh. Yulaeva[2]

[1]L.N. Gumilyov Eurasian National University, Nur-Sultan, Kazakhstan

[2]Bashkir State University, Ufa, Russia

E-mail: kubenova.m@yandex.kz

DOI: **10.29317/ejpfm.2020040108**
Received: 11.02.2020 - after revision

Nanocrystalline alloys of the compositions $Na_{0.05}Cu_{1.95}S$, $Na_{0.075}Cu_{1.925}S$, $Na_{0.10}Cu_{1.90}S$, $Na_{0.125}Cu_{1.750}S$, $Na_{0.15}Cu_{1.85}S$, $Na_{0.17}Cu_{1.80}S$, $Na_{0.20}Cu_{1.77}S$ were synthesized in a melt medium mixtures of hydroxides NaOH and KOH at a temperature of about 165 ° C. X-ray phase analysis showed that the alloys are heterophasic and consist of phases of Cu_9S_5 digenite, CuS_2 copper disulfide, Covellite CuS, Cu_7S_4 anilite in various combinations. The crystallite sizes range from 16 to 160 nm. The degree of crystallinity of the alloys slightly increases with an increase in the sodium content from 68% in $Na_{0.05}Cu_{1.95}S$ to 81% in $Na_{0.20}Cu_{1.77}S$. A quasi-one-dimensional $Na_2Cu_4S_3$ phase was detected in the composition of the $Na_{0.20}Cu_{1.77}S$ alloy. The measured values of the conductivity of the alloys are two orders of magnitude lower than in isolated pure Cu_9S_5, CuS_2, CuS, Cu_7S_4, of which the alloys consist. An activation temperature dependence of the conductivity is observed in the region from 300 K to 360 K with an activation energy of 0.08 - 0.15 eV. The reason for the low conductivity of the alloys is assumed to be the presence of weakly conducting interfacial layers and sodium doping of non-stoichiometric phases Cu_9S_5 ($Cu_{1.8}S$) and Cu_7S_4 ($Cu_{1.75}S$), leading to the compensation of holes by electrons of impurity sodium atoms. The measured values of the coefficient of thermo-emf alloys at room temperature lie in the range from 0.032 to 0.147 mV/K. Due to the low thermal conductivity of the order of 0.2 W/mK, a rather high dimensionless thermoelectric figure of merit ZT $\approx$ 0.28 at 570 K was obtained for the composition $Na_{0.15}Cu_{1.85}S$.

Keywords: thermoelectric materials, thermoelectric generators, synthesis, solid chalcogenides, nanopowders.

Introduction

$Cu_{2-\delta}S$ copper sulfide is a superionic semiconductor compound of variable composition, which has recently attracted great attention of researchers with the prospects of using it as a thermoelectric material. The object of this interest is the very low lattice thermal conductivity (λ) of copper sulfide in the superionic phase with high electronic conductivity (σ_e) and Seebeck coefficient (α_e), which provides high thermoelectric figure of merit ZT = $\sigma_e\alpha_e 2T/\lambda$, lying in the range 0.4-1.9 depending on chemical composition and method of sample preparation [1-4].

Copper sulfide is part of a separate class of superionic thermoelectric materials recently identified among thermoelectrics [5], which are characterized by the effect of the "phonon-liquid electron crystal" [6], which consists in suppressing the propagation of phonons by the "crystal" melt in the superionic state of the material lattice.

This work is a continuation of a series of studies on the study of alloys of copper sulfide with alkali metals and the effect of sodium on the electrophysical, including thermoelectric, properties of alloys.

Recently, Guan M.J. et al. [7] studied $Cu_{2-x}Li_xS$ samples (x = 0, 0.005, 0.010, 0.050, and 0.100) obtained by fusion-quenching-annealing. With lithium contents up to x = 0.05, the samples they obtained were single-phase at room temperature and had a monoclinic structure similar to pure Cu_2S, which can be considered as the formation of a lithium solid solution in copper sulfide. It was found that the electrical conductivity of $Cu_{2-x}Li_xS$ increases by an order of magnitude or more with increasing lithium content, which Guan M.J. et al. explained by an increase in carrier concentration. However, as expected, the Seebeck coefficient decreases simultaneously, but decreases 2-3 times weaker than the conductivity increases. Interestingly, doping with lithium leads to an increase in not only electronic, but also lattice thermal conductivity. The maximum thermoelectric figure of merit (ZT = 0.84) was observed by Guan M.J. et al. for the composition $Cu_{1.99}Li_{0.01}S$ at 900 K, which is a third higher than the ZT value for pure copper sulfide obtained by the same method.

It is possible that it would be more promising to choose a non-stoichiometric composition of copper sulfide for alloying in order to have an initially large concentration of holes, since the conductivity of the stoichiometric composition is too low to obtain a high thermoelectric power of the material. This consideration was one of the reasons for the inclusion of non-stoichiometric compositions in the series of samples for our study.

In [7-10], the effect of doping with lithium and potassium on the thermoelectric properties of copper sulfide is reported. The effect of doping with sodium on transport phenomena in copper sulfide was studied in [11]. Z.H. Ge et al [11] described the thermoelectric properties of bulk samples of $Na_xCu_9S_5$ copper sulfide (x = 0, 0.025, 0.05, 0.15, 0.25), consolidated using spark plasma sintering technology from nanopowder with an average nanoparticle size of 3 nm, synthesized by mechanical alloying, and the solubility of sodium in the crystal structure of copper sulfide to a composition of x = 0.05 is shown. The purpose of

the doping was to reduce conductivity and increase the Seebeck coefficient. Z.H. Ge et al showed by Hall effect measurements that doping with sodium is expected to reduce the concentration of carriers in Cu_9S_5. In addition, the presence of many nanoscale pores and grains was found, which led to a decrease in thermal conductivity by a factor of 2-3. As a result, they achieved a high value of ZT = 1.1 at 500 °C for $Na_{0.05}Cu_9S_5$, mainly due to a decrease in thermal conductivity. The solubility of sodium in the interstices of the Cu_9S_5 lattice is 0.28%; at a higher sodium concentration (for the $Na_{0.25}Cu_9S_5$ alloy), the formation of inclusions of the Na_2S and $Cu_{1.96}S$ phases is noted.

In this work, we study the phase composition, electrical conductivity, thermal conductivity, Seebeck coefficient of semiconductor nanocrystalline alloys $Na_{0.05}Cu_{1.95}S$; $Na_{0.075}Cu_{1.925}S$; $Na_{0.10}Cu_{1.90}S$; $Na_{0.125}Cu_{1.750}S$, $Na_{0.15}Cu_{1.85}S$; $Na_{0.17}Cu_{1.80}S$; $Na_{0.20}Cu_{1.77}S$ in order to study the prospects of their practical use as thermoelectric materials.

The experimental procedure

The investigated alloys of the compositions $Na_{0.05}Cu_{1.95}S$, $Na_{0.075}Cu_{1.925}S$, $Na_{0.10}Cu_{1.90}S$, $Na_{0.125}Cu_{1.750}S$, $Na_{0.15}Cu_{1.85}S$, $Na_{0.17}Cu_{1.80}S$, $Na_{0.20}Cu_{1.77}S$ were synthesized according to the procedure, similar to that described in [10] in a melt medium of a mixture of NaOH and KOH hydroxides at a temperature of about 165 °C. All reagents (CuCl, NaCl, Na_2S*$9H_2O$) were placed in a heated Teflon reactor at the same time. After laying the reagents, the exposure time was 16 hours. The product obtained as a precipitate was washed three times with distilled heated water, then with pure ethanol. The washed powder was dried at 50 °C. The particle sizes of the obtained powder were in the range from 15 to 100 nm.

X-ray phase analysis of the samples was carried out on a D8 ADVANCE ECO diffractometer (Bruker, Germany) using CuK_α radiation. To identify the phases and study the crystal structure, Bruker AXSDIFFRAC.EVAv.4.2 software and the ICDD PDF-2 international database were used.

To measure the transport characteristics of the powder, samples in the form of parallelepipeds ($2 \times 5 \times 20$) mm in size were pressed under a pressure of (3-5) t/cm^2. Samples were annealed in argon at 500 °C for 8 hours.

The electrical conductivity and thermo-emf of the $Na_xCu_{2-x}S$ samples were studied at the ZEM-3 experimental setup (Japan). The setup software corrects for the contribution of metal wires to the measured thermo-emf, since it can introduce a significant error in the study of samples with a low Seebeck coefficient.

The thermal diffusivity and thermal conductivity of solid samples were measured on an LFA 467 HT HyperFlash instrument (NETZSCH, Germany). The thermal diffusivity was determined by the Parker formula:

$$a = 0.1388\frac{l^2}{t_{1/2}}, \quad (1)$$

where, a is the thermal diffusivity, l - is the thickness of the sample, $t_{1/2}$ - is the time in s, corresponding to a temperature increase of 50%.

Thermal conductivity (λ) was defined as

$$\lambda(T) = a(T) * \rho(T) * c_P(T), \quad (2)$$

where, T – is temperature, a – is thermal diffusivity, ρ – is bulk density, c_P – is specific heat.

The density of the sample was determined from measurements of the weight and volume of the sample. The values of c_P were determined using a DSC-calorimeter DSC 404 F1 Pegasus company NETZSCH (Germany).

The results of the experiment and their discussion

Phase analysis

X-ray diffraction patterns of samples taken at room temperature are shown in Figure 1.

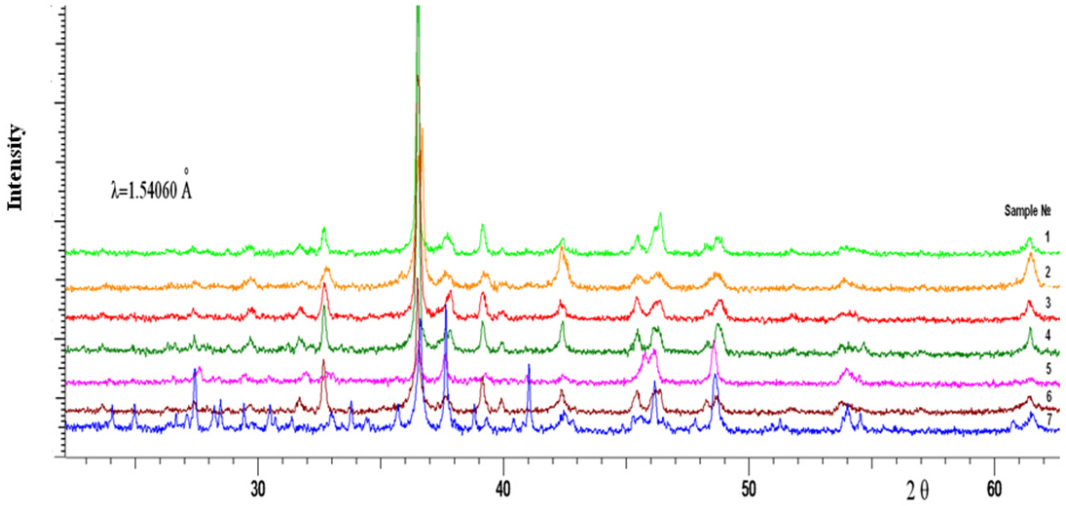

Figure 1. X-ray diffraction patterns of samples taken at room temperature: 1) $Na_{0.05}Cu_{1.95}S$; 2) $Na_{0.075}Cu_{1.925}S$; 3) $Na_{0.10}Cu_{1.90}S$; 4) $Na_{0.125}Cu_{1.750}S$; 5) $Na_{0.15}Cu_{1.85}S$; 6) $Na_{0.17}Cu_{1.80}S$; 7) $Na_{0.20}Cu_{1.77}S$.

Tables 1-7 below show the phase composition of the samples and estimates of their crystallinity, crystallite size, and percentage of phases obtained from the analysis of diffractograms shown in Figure 1.

As can be seen from the results of the analysis, all samples contained a significant fraction of Cu_9S_5 digenite (from 22 to 52%).

At a sodium content in the samples with $x \leq 0.125$, the CuS_2 phase is present, which prevails in $Na_{0.05}Cu_{1.95}S$ (78%) and almost disappears in the $Na_{0.125}Cu_{1.875}S$ sample (2%). In samples with $x>0.125$, the CuS_2 phase does not form.

The crystallite sizes range from 16 to 160 nm.

The degree of crystallinity increases slightly with increasing sodium content from 68% for $Na_{0.05}Cu_{1.95}S$ to 81% for $Na_{0.20}Cu_{1.77}S$.

At the highest sodium content in the alloy (the chemical composition of $Na_{0.20}Cu_{1.77}S$), the $Na_2Cu_4S_3$ phase appears, which differs from other phases in its quasi-one-dimensional crystalline structure [12]. No other compounds

Table 1.
The results of x-ray phase analysis of $Na_{0.05}Cu_{1.95}S$ at room temperature.

Phase	Structure type	Space group	(hkl)	$2\theta°$	d, Å	L, nm	Cell parameter, Å	Degree of crystallinity, %	FWHM	Phase Content, %
Cu_9S_5– digenite (PDF 00-047-1748)	Rhombo.H.axes	R-3m(225)	1010	32.684	2.73766	46.91	a=3.84956, c=48.14446	65.5	0.196	22.3
			1013	36.476	2.46130	69.41			0.134	
			0114	37.684	2.38510	42.71			0.218	
			0117	42.398	2.13022	49.57			0.191	
			0120	46.356	1.95713	26.16			0.367	
			119	48.682	1.86890	16.47			0.588	
			2017	61.447	1.50774	41.84			0.245	
CuS_2– Copper Sulfide (PDF 01-082-6358)	Orthorhombic	Pnn2(34)	200	31.687	2.82149	48.23	a=4.66907, b=5.79055, c=3.55557	65.5	0.190	77.7
			211	39.150	2.29913	53.28			0.176	
			220	45.480	1.99277	50.29			0.190	

Table 2.
The results of x-ray phase analysis Na)0.075 Cu $_{1.925}$ Sroom temperature.

Phase	Structure type	Space group	(hkl)	2θ°	d, Å	L, nm	Cell parameter, Å	Degree of crystallinity, %	FWHM	Phase Content, %
Cu_9S_5– digenite (PDF 00-047-1748)	Rhombo.H.axes	R-3m(225)	107	29.461	3.02945	23.28	*a*=3.86396, *c*=47.66778	67.5	0.392	31.7
			1010	32.598	2.74468	27.11			0.339	
			1014	36.468	2.46182	30.60			0.304	
			0114	37.462	2.39872	48.15			0.194	
			0117	42.238	2.13792	26.35			0.359	
			0120	46.177	1.96429	29.60			0.324	
			119	48.443	1.87757	17.79			0.544	
CuS_2– Copper Sulfide (PDF 01-082-6358)	Orthorhombic	Pnn2(34)	211	39.048	2.30590	28.23	*a*=4.62823, *b*=5.76230, *c*=3.54514	67.5	0.332	68.3
			220	45.305	2.00003	44.26			0.216	
			311	53.637	1.70734	68.76			0.144	
			2013	61.272	1.51163	30.23			0.339	

Table 3.
The results of x-ray phase analysis $Na_{0.1}Cu_{1.9}S$ room temperature.

Phase	Structure type	Space group	(hkl)	$2\theta^{\circ}$	d, Å	L, nm	Cell parameter, Å	Degree of crystallinity, %	FWHM	Phase Content, %
Cu_9S_5– digenite (PDF 00-047-1748)	Rhombo.H.axes	R-3m(225)	0114	37.879	2.37329	37.39	a=3.88299, c=47.39826	75.1	0.250	31.5
			1110	46.357	1.95706	25.13			0.382	
			119	48.844	1.86307	24.24			0.400	
CuS – Covellite (PDF 01-078-0877)	Hexagonal	P63/mmc(194)	006	32.746	2.73264	41.39	a=3.77350, c=16.38830	75.1	0.222	25.9
			106	42.340	2.13300	43.90			0.216	
			107	48.270	1.88388	74.46			0.130	
			116	61.455	1.50757	38.00			0.270	
CuS_2– Copper Sulfide (PDF 01-082-6358)	Orthorhombic	127	111	27.390	3.25356	71.61	a=4.64371, b=5.77930, c=3.55001	75.1	0.127	42.6
			210	36.525	2.45814	44.12			0.211	
			211	39.138	2.29982	37.56			0.249	
			220	45.461	1.99356	41.79			0.229	

Table 4.
The results of x-ray phase analysis $Na_{0.125}Cu_{1.750}S$ room temperature.

Phase	Structure type	Space group	(hkl)	$2\theta^{\circ}$	d, Å	L, nm	Cell parameter, Å	Degree of crystallinity, %	FWHM	Phase Content, %
Cu_9S_5– digenite (PDF 00-047-1748)	Rhombo.H.axes	R-3m(225)	0120	46.194	1.96361	23.94	*a*=3.90674, *c*=47.59424	79.3	0.401	49.5
CuS – Covellite (PDF 01-078-0877)	Hexagonal	P63/mmc(194)	102	29.669	3.00863	43.10	*a*=3.81162, *c*=16.45606	79.3	0.212	15.2
Cu_7S_4– Anilite (PDF 01-072-0617)	Orthorhombic	Pnma(62)	004	32.689	2.73731	58.00	*a*=7.84357, *b*=7.82594, *c*=10.97963	79.3	0.159	32.8
			114	36.503	2.45951	103.77			0.090	
			302	37.666	2.38621	39.40			0.237	
			033	42.420	2.12917	53.73			0.176	
			225	48.723	1.86741	30.01			0.323	
			306	61.433	1.50805	58.92			0.174	
CuS_2– Copper Sulfide (PDF 01-082-6358)	Orthorhombic	Pnn2(34)	111	27.384	3.25425	102.27	*a*=4.64644, *b*=5.80777, *c*=3.53269	79.3	0.087	2.5
			200	31.648	2.82488	51.78			0.177	
			211	39.094	2.30227	61.68			0.152	
			220	45.439	1.99446	67.36			0.142	
			311	53.783	1.70307	35.44			0.280	

Table 5.
The results of x-ray phase analysis $Na_{0.15}Cu_{1.85}S$ room temperature.

Phase	Structure type	Space group	(hkl)	2θ°	d, Å	L, nm	Cell parameter, Å	Degree of crystallinity, %	FWHM	Phase Content, %
Cu_9S_5– digenite (PDF 00-047-1748)	Rhombo.H.axes	R-3m(225)	203	33.227	2.69418	42.10	*a*=3.92444, *c*=47.77221	78.4	0.219	52.2
			311	36.981	2.42882	51.33			0.181	
			302	38.037	2.36382	57.50			0.162	
CuS – Covellite (PDF 01-078-0877)	Hexagonal	P63/mmc(194)	100	26.966	3.30383	145.70	*a*=3.81836, *c*=16.36302	78.4	0.062	13
Cu_7S_4– Anilite (PDF 01-072-0617)	Orthorhombic	Pnma(62)	022	28.036	3.18012	63.03	*a*=7.86671, *b*=7.78169, *c*=10.93460	78.4	0.144	20.2
			004	32.394	2.76132	33.48			0.275	
			106	42.812	2.11056	41.14			0.230	
			040	46.394	1.95562	15.24			0.631	
			402	48.954	1.85915	46.06			0.211	
			035	54.404	1.68508	16.37			0.606	
S – Sulfur (PDF 01-076-0183)	Monoclinic	P2(3)	334	39.715	2.26771	35.92	*a*=17.53547, *b*=9.16498, *c*=13.68934, beta = 113.111°	78.4	0.261	14.6

Table 6.
The results of x-ray phase analysis $Na_{0.17}Cu_{1.80}S$ room temperature.

Phase	Structure type	Space group	(hkl)	2θ°	d, Å	L, nm	Cell parameter, Å	Degree of crystallinity, %	FWHM	Phase Content, %
Cu_9S_5– digenite (PDF 00-047-1748)	Rhombo.H.axes	R-3m(225)	101	26.059	3.41670	68.39	*a*=3.91906, *c*=48.06437	77.5	0.132	47
			107	29.381	3.03751	35.46			0.257	
			0120	46.139	1.96581	21.32			0.450	
CuS – Covellite (PDF 01-078-0877)	Hexagonal	P63/mmc(194)	100	27.216	3.27403	34.96	*a*=3.79825, *c*=16.45011	77.5	0.260	19.8
			105	38.950	2.31047	61.08			0.153	
Cu_7S_4– Anilite (PDF 01-072-0617)	Orthorhombic	Pnma(62)	020	23.464	3.78833	92.24	*a*=7.84304, *b*=7.78169, *c*=10.94963	77.5	0.098	29.5
			004	32.471	2.75511	51.43			0.179	
			114	36.289	2.47354	61.56			0.151	
			302	37.479	2.39770	29.47			0.316	
			132	39.727	2.26707	62.48			0.150	
			321	42.189	2.14026	55.44			0.171	
			234	53.660	1.70963	21.73			0.455	
			502	61.212	1.51297	34.27			0.299	
S – Sulfur (PDF 01-076-0183)	Monoclinic	P2(3)	303	31.496	2.83815	57.03	*a*=17.55957, *b*=9.17037, *c*=13.74054, beta = 112.494°	77.5	0.161	3.7
			440	45.247	2.00248	39.13			0.244	
			517	48.056	1.88176	74.88			0.129	

Table 7.
The results of x-ray phase analysis $Na_{0.20}Cu_{1.77}S$ room temperature.

Phase	Structure type	Space group	(hkl)	2θ°	d, Å	L, nm	Cell parameter, Å	Degree of crystallinity, %	FWHM	Phase Content, %
Cu_9S_5– digenite (PDF 00-047-1748)	Rhombo.H.axes	R-3m(225)	1013	35.683	2.51413	62.71	*a*=3.94926, *c*=48.18720	81.1	0.141	51
			0120	46.145	1.96557	72.89			0.132	
$Na_2Cu_4S_3$ - sodium Copper Sulfide (PDF 01-082-6340)	Monoclinic	C2/m(12)	111	25.933	3.56269	120.29	*a*=15.85255, *b*=3.87733, *c*=11.85103, beta=95.831°	81.1	0.075	18.5
			402	28.222	3.15950	76.07			0.120	
			311	29.424	3.03316	138.50			0.066	
			204	31.358	2.85035	98.21			0.093	
			601	33.796	2.65008	81.24			0.114	
			114	39.323	2.28941	75.50			0.124	
			512	41.029	2.19809	95.63			0.099	
CuS – Covellite (PDF 01-078-0877)	Hexagonal	P63/mmc(194)	100	27.097	3.28809	71.65	*a*=3.79008, *c*=16.38265	81.1	0.127	2.3
			006	33.005	2.71178	49.99			0.184	
			105	38.825	2.31763	95.80			0.098	
Cu_7S_4 – Anilite (PDF 01-072-0617)	Orthorhombic	Pnma(62)	121	26.663	3.34059	162.24	*a*=7.85751, *b*=7.82002, *c*=10.98625	81.1	0.056	12.9
			212	30.485	2.92998	97.21			0.115	
			114	36.615	2.45226	47.95			0.194	
			302	37.647	2.38740	88.32			0.106	
			223	40.419	2.22982	88.14			0.107	
			033	42.453	2.12759	41.94			0.226	
			225	48.613	1.87141	40.71			0.238	
			413	53.993	1.69694	58.41			0.170	
S – Sulfur (PDF 01-076-0183)	Monoclinic	P2(3)	410	24.057	3.69625	146.30	*a*=17.53550, *b*=9.20466, *c*=13.77024, beta=113.003°	81.1	0.062	15.3
			520	27.431	3.24880	71.73			0.121	
			323	28.469	3.13273	112.47			0.081	
			503	30.684	2.91141	136.97			0.067	

containing sodium were detected, although energy dispersive analysis showed an approximately uniform distribution of sodium in all samples.

Also in some alloys there are phases CuS, Cu_7S_4 and sulfur inclusions.

The DTA curves (Figure 2) obtained on a DSC - DSC 404 F1 calorimeter show sharp exothermic peaks of about (360-370) K, reflecting the phase transition from the rhombohedral modification of digenite to cubic modification.

It is known that copper disulfide at atmospheric pressure is stable only below 200 ° C [13]. There is evidence that, at a temperature of 220 ° C, the melting of covellite CuS and its decomposition with the formation of copper sulfide Cu_2S begins [12]. On the other hand, works [14-15] testify to the stability of covellite up to 507 ° C when it transforms into cubic digenite.

A sharp decrease in the DTA curve above 200 ° C in Figure 2 can be related to the ongoing decomposition of CuS_2 and the formation of Cu_2S.

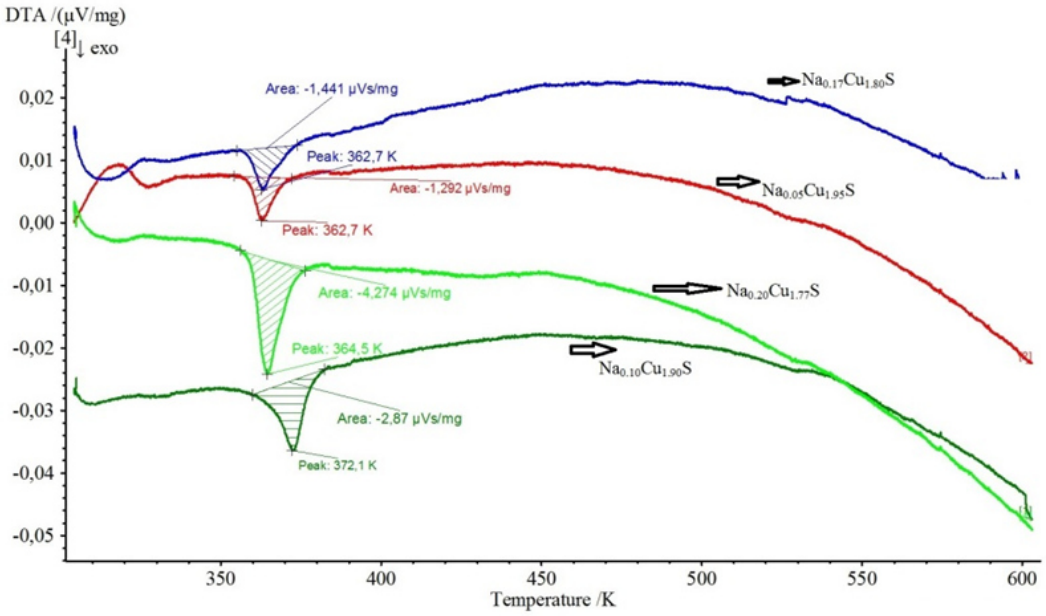

Figure 2. Curves of differential thermal analysis of samples: $Na_{0.05}Cu_{1.95}S$, $Na_{0.10}Cu_{1.90}S$, $Na_{0.17}Cu_{1.80}S$, $Na_{0.20}Cu_{1.77}S$.

Electronic conductivity

Figure 3 shows the temperature dependences of the electronic conductivity of the samples under study in the temperature range (300-600) K.

Since the alloys are heterophase at room temperature, it is difficult to interpret the obtained dependences, however, based on the analysis, certain assumptions can be made in order to have a working hypothesis for further research.

The anomalies in the behavior of the temperature dependence of about (360-400) K for all compositions can be attributed to the manifestation of the superionic phase transition (FP) in digenite, which takes place at 364 K for diagenite of the Cu_9S_5 composition [16]. Digenite is present as a separate phase in all samples, according to the results of x-ray phase analysis. The scatter in the temperature values of the phase transitions for different compositions can be explained by the effect of dissolved sodium and the influence of non-stoichiometry, which is difficult to control for sulfides.

The lowest conductivity values (below 5 S/cm) are observed for the $Na_{0.075}Cu_{1.925}S$ alloy, the highest values (from 47 to 68 S/cm) for $Na_{0.05}Cu_{1.95}S$.

According to the work of R.A. Munson et al [17], copper disulfide at room temperature has a conductivity of about 500 S/cm, therefore, the presence of this phase in the alloy should increase the conductivity. This assumption is consistent with the fact that the $Na_{0.05}Cu_{1.95}S$ sample has the highest conductivity of all alloys, in which the copper disulfide content is maximum (78%), and the highly conductive Cu_9S_5 digenite is also the second phase in it. The conductivity of digenite at room temperature is even higher than that of copper disulfide and is more than 3000 S/cm at room temperature [3]. In our case, when the observed conductivity of the alloys is much lower than 3000 S/cm, it can be assumed that the content of digenite does not exceed the percolation threshold, and the crystallites of digenite are separated by a weakly conducting medium.

Copper disulfide exhibits a metallic character of conductivity in the range of (0-300) K [18] at a temperature of 1.6 K and becomes superconducting. Judging by the fact that the studied alloys exhibit a semiconductor rather than metallic character of conductivity near room temperature, copper disulfide does not determine the conductivity of the alloy, apparently because its content in the samples is small.

Covellite CuS also exhibits excellent metallic properties, its conductivity decreases from 10100 S/cm at 320 K to 6200 S/cm at 580 K, the coefficient of thermo-emf in this case, it increases from 9 to 11.2 μV/K [19]. The covellite phase is present in all samples except $Na_{0.05}Cu_{1.95}S$ and $Na_{0.075}Cu_{1.925}S$, its relative content is from 2 to 25%, however, its presence also does not determine the electrical and thermoelectric properties of the alloy.

Presumably, in the crystallites of digenite and copper disulfide there is sodium dissolved in the lattice, which plays the role of a compensating impurity. It is known that doping with sodium reduces the concentration of digenite holes [11] formed during ionization of vacancies in the copper sublattice; in addition, carrier mobility is reduced due to scattering of impurity (Na) ions. An additional factor in reducing the mobility of carriers is scattering at the boundaries of nanocrystallites, so the specific surface fraction increases significantly with decreasing grain size. Numerous interphase boundaries also lead to a decrease in conductivity.

We also take into account that, according to Roseboom [20], the copper content in digenite increases with temperature, reaching a composition close to stoichiometric (Cu_2S) at 708 K. The conductivity of stoichiometric copper sulfide is 0.07 $S \cdot cm^{-1}$ according to the work of Okamoto and Kawai [21].

The fraction of digenite in the phase composition of our samples is 22-52%, therefore, a significant decrease in the conductivity of alloys with increasing temperature can be attributed to a decrease in the hole concentration due to an increase in the copper content in digenite. This may be the reason for a sharp decrease in conductivity above 550 K in the alloys $Na_{0.15}Cu_{1.85}S$, $Na_{0.17}Cu_{1.80}S$, $Na_{0.20}Cu_{1.77}S$, for which n in the ratio $\sigma \approx T^{-n}$ is several times greater than 3/2, i.e., the a decrease in mobility due to an increase in scattering due to thermal vibrations of the lattice is not able to explain such a sharp decrease in conductivity with temperature.

For the temperature range up to 360 K, in which the semiconductor nature

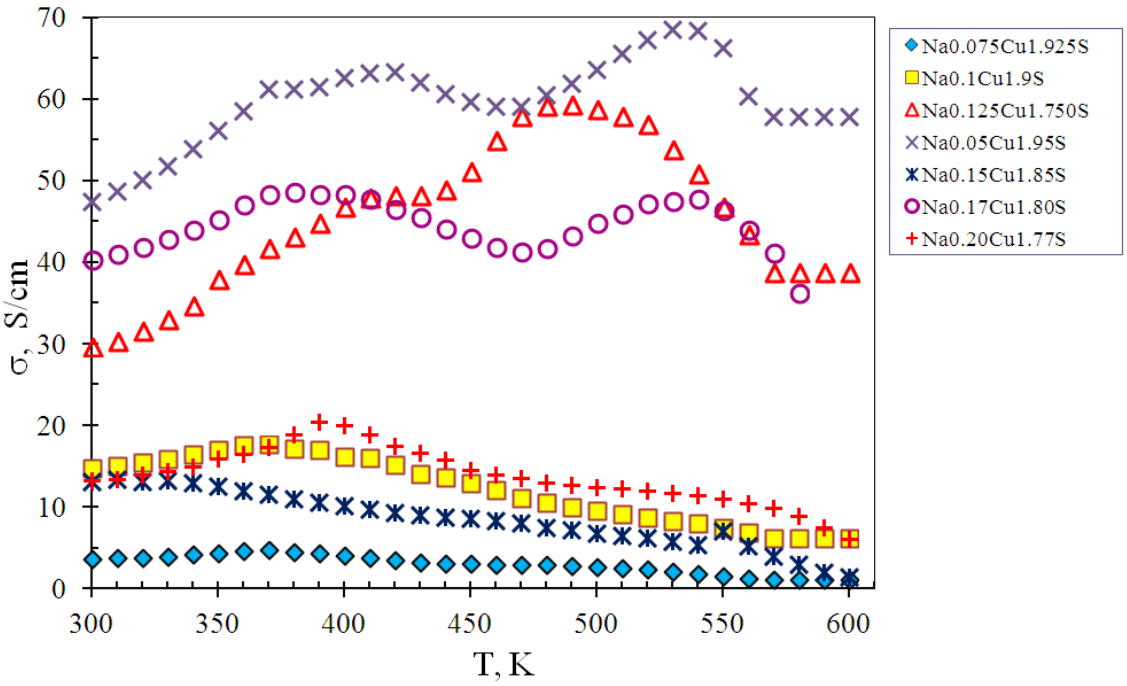

Figure 3. Temperature dependences of electronic conductivity.

of the temperature dependence of the conductivity in Figure 3 is observed, the activation energy of conductivity can be determined. The results are shown in Table 8.

The presence of activation thermal conductivity can be related to the fact that current carriers overcome energy barriers during transitions between conductive crystallites in an essentially nanocomposite material.

For comparison, we note that in the low-temperature phase of copper sulfide (jarleite $Cu_{1.92}S$) in the work of G.P. Sorokin and A.P. Paradenko [22], the activation energy of electronic conductivity 0.09 eV was obtained.

Thus, the electrical properties of the studied alloys differ from the properties of the metal-like phases Cu_9S_5, CuS, CuS_2 included in their composition. The reason may be the presence of weakly conducting interfacial layers and sodium doping of non-stoichiometric Cu_9S_5 ($Cu_{1.8}S$), which leads to the compensation of holes by electrons of impurity sodium atoms.

Electronic thermo-emf

Temperature dependences of the coefficient of electronic thermo-emf samples are presented in Figure 4. The sign of the coefficient is positive for all samples, which corresponds to the hole type conductivity. In general, with increasing temperature, there is a tendency to increase the coefficient of electronic thermo-emf.

The coefficient of thermo-emf increases most strongly above 550 K, the only exception is the alloy $Na_{0.17}Cu_{1.80}S$, which has a coefficient of thermo-emf varies slightly between 0.09 and 0.10 mV/K in a wide range of (400-600) K.

In general, the coefficient of thermo-emf in all samples is higher than in pure nanocrystalline $Cu_{1.8}S$ (Cu_9S_5), for which the measurement results from [3] are also shown in Figure 4.

Thermal conductivity

Figure 5 shows the temperature dependence of the thermal conductivity of the

Table 8.
Values of activation energy of conductivity of alloys in the temperature range 300-360 K.

Alloy	$Na_{0.05}Cu_{1.95}S$	$Na_{0.075}Cu_{1.925}S$	$Na_{0.1}Cu_{1.9}S$	$Na_{0.125}Cu_{1.750}S$	$Na_{0.17}Cu_{1.80}S$	$Na_{0.20}Cu_{1.77}S$
E_a, eV	0.15±0.01	0.08±0.01	0.11±0.01	0.15±0.01	0.13±0.01	0.11±0.01

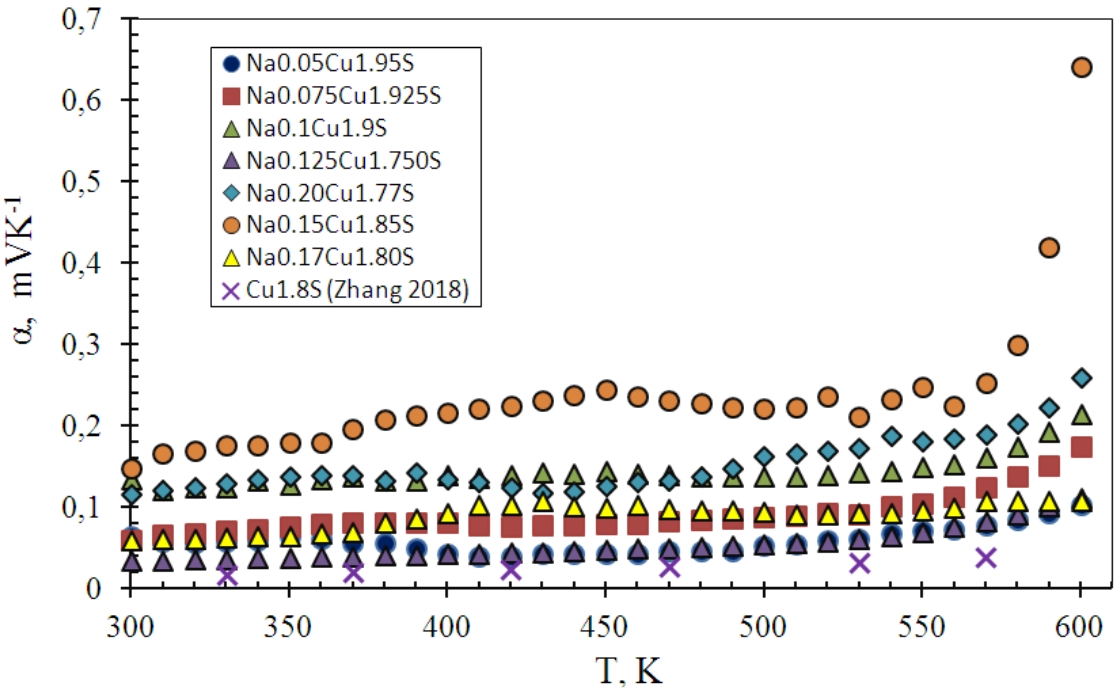

Figure 4. Temperature dependences of the coefficient of electronic thermo-emf.

samples in the temperature range from room temperature to 610 K.

Very low values of thermal conductivity are observed (up to 0.1 $Wm^{-1}K^{-1}$), which is a favorable factor for the use of this material for thermoelectric purposes. Low thermal conductivity is associated with the "moltenness" of the cationic sublattice of the material, which leads to the suppression of phonon thermal conductivity, as well as nanoscale crystallites and multiphase material, causing additional structural defects on which phonon scattering occurs.

In a recent paper [11], low thermal conductivity was also observed for nanocrystals of copper sulfide doped with sodium; however, for our samples, the thermal conductivity in the range from 300 to 500 K turned out to be several times lower, apparently due to the much lower electronic component of thermal conductivity.

Thermoelectric efficiency

The kinetic parameters were used to determine the dimensionless thermoelectric figure of merit ZT = $\sigma_e\ \alpha_e^2$ T/k shown in Figure 6. The maximum ZT = 0.28 at 570 K was obtained for the $Na_{0.15}Cu_{1.85}S$ alloy. This is significantly higher than ZT $\approx$0.2 at the same temperature for sodium doped Cu_9S_5, achieved by Z.H. Ge et al [11].

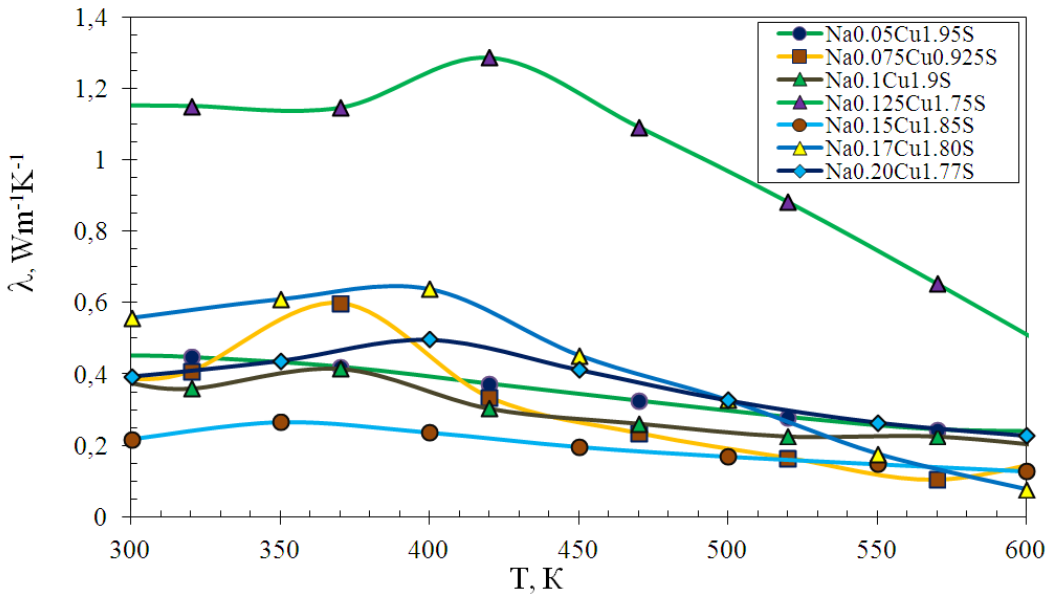

Figure 5. Temperature dependences of thermal conductivity.

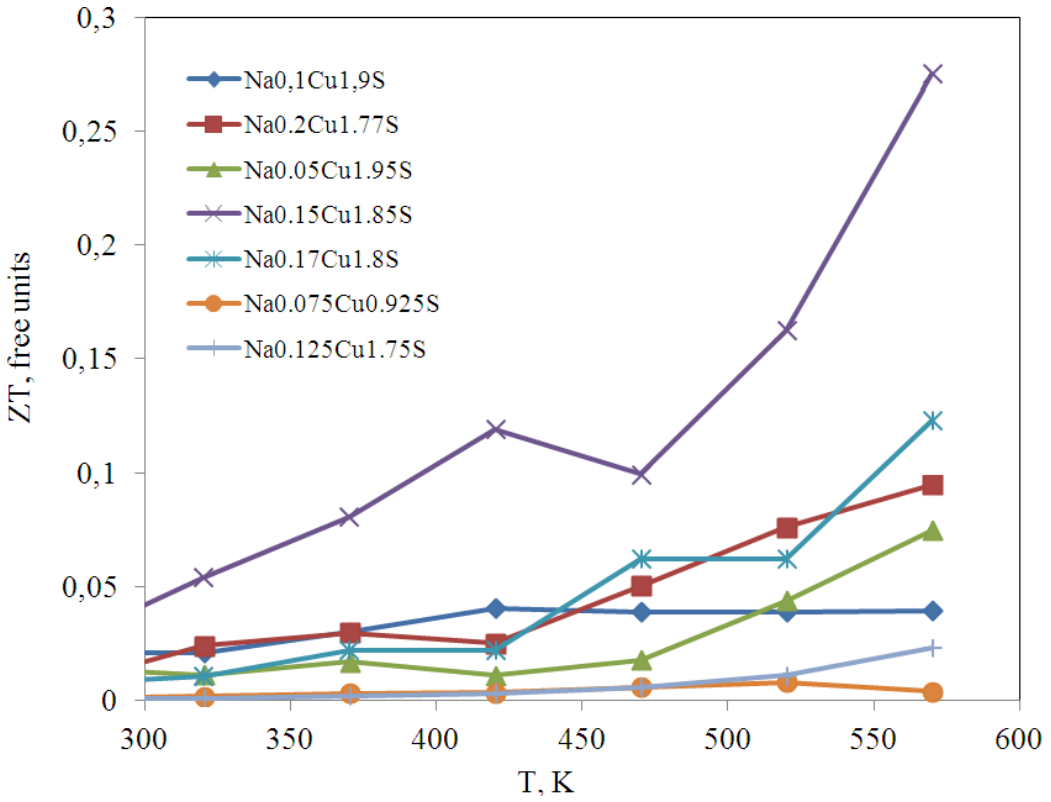

Figure 6. Temperature dependences of thermoelectric figure of merit.

Conclusion

The resulting alloys are $Na_{0.05}Cu_{1.95}S$, $Na_{0.075}Cu_{1.925}S$, $Na_{0.10}Cu_{1.90}S$, $Na_{0.125}Cu_{1.750}S$; $Na_{0.15}Cu_{1.85}S$, $Na_{0.17}Cu_{1.80}S$, $Na_{0.20}Cu_{1.77}S$ are heterophasic, consisting of a mixture of nanosized crystallites of digenite Cu_9S_5, copper disulfide CuS_2, covellite CuS, anilite Cu_7S_4. Some samples showed small sulfur inclusions. Only at the highest sodium content in the alloy (chemical composition of $Na_{0.20}Cu_{1.77}S$) $Na_2Cu_4S_3$ phase appears, which differs from other phases in

its quasi-one-dimensional crystalline structure. No other compounds containing sodium were detected, although energy dispersive X-ray analysis showed an approximately uniform distribution of sodium in all samples.

All samples contain a significant proportion of Cu_9S_5 digenite (from 22 to 52%), other phases may be absent.

The crystallite sizes range from 16 to 160 nm. The degree of crystallinity of the alloys slightly increases with an increase in the sodium content from 68% for $Na_{0.05}Cu_{1.95}S$ to 81% for $Na_{0.20}Cu_{1.77}S$.

The electrical properties of the studied alloys are very different from the properties of the metallic phases Cu_9S_5, Cu_7S_4, CuS, CuS_2 included in their composition. The measured values of the conductivity of the alloys are two orders of magnitude lower than in the pure substances listed above; for the studied alloys, an activation temperature dependence of the conductivity is observed in the region from 300 K to 360 K with an activation energy of (0.08-0.15) eV. The low conductivity of the alloys can be caused by the presence of weakly conducting interfacial layers and sodium doping of non-stoichiometric phases Cu_9S_5 ($Cu_{1.8}S$) and Cu_7S_4 ($Cu_{1.75}S$), which leads to the compensation of holes by electrons of impurity sodium atoms.

Sign of the coefficient of thermo-emf corresponds to the hole type of conductivity, the values of the coefficient of thermo-emf at room temperature, they range from 0.032 mV/K for $Na_{0.125}Cu_{1.750}S$ to 0.147 mV/K for $Na_{0.15}Cu_{1.85}S$.

The composition of $Na_{0.15}Cu_{1.85}S$ exhibits high values of electronic conductivity, coefficient of electronic thermo-emf and low thermal conductivity at the level of 0.2 W/mK, which gives a rather high indicator of dimensionless thermoelectric figure of merit $ZT \approx 0.28$ at 570 K and allows us to hope in the future for the possibility of increasing this indicator due to the optimization of the synthesis procedure.

Acknowledgments

This research was supported by the Ministry of Education and Science of the Republic of Kazakhstan in the framework of scientific and technology Program BR05236795 "Development of Hydrogen Energy Technologies in the Republic of Kazakhstan".

References

[1] Y.Q. Tang et al., Crystals **7**(141) (2017) 1-10.
[2] L.J. Zheng et al., Alloys and Compounds **722** (2017) 17-24.
[3] Y.-X. Zhang et al., Journal of Alloys and Compounds **764** (2018) 738-744.
[4] Z.-H. Ge et al., Mat. Today Phys. **8** (2019) 71-77.
[5] P. Qiu et al., Energy Storage Materials **3** (2016) 85-97.
[6] H. Liu et al., Nat. Mater. **11** (2012) 422-425.
[7] M.J. Guan et al., Rare Met. **37** (2018) 282-289.
[8] M.Kh. Balapanov et al., Inorganic Materials **50**(9) (2014) 930-933.

[9] R.Kh. Ishembetov et al., Rus. J. Electrochem. **47** (2011) 416-419.
[10] X.Y. Li et al., J. Mater. Chem. A. **1**(44) (2013) 13721.
[11] Z.H. Ge et al., Adv. En. Mat. **6** (2016) 1600607.
[12] G. Savelsberg, H. Schafer, Materials Research Bulletin **16**(10) 1291-1297.
[13] Ju.D. Tret'jakova, Himija perehodnyh jelementov (M.: Izdatel'skij centr «Akademija», 2007) 400 p. (in Russian)
[14] R.W. Potter, Economic Geology **72** (1977) 1524-1542.
[15] E.F. Westrum et al., The Journal of Chemical Thermodynamics **19**(11) (1987) 1199-1208.
[16] D.J. Chakrabarti et al., J. Phase Equilibria (1983) **4**(3) 254-271.
[17] R.A. Munson et al., The Journal of Chemical Physics **47**(5) (1967) 1769-1770.
[18] T.A. Bither et al., Inorganic Chemistry **7**(11) (1968) 2208-2220.
[19] G. Dennler et al., Adv. Energy Mater. (2014) 1301581.
[20] E.H. Roseboom, Econ. Geol. **61** (1966) 641-672.
[21] K. Okamoto, Sh. Kawai, Japan Journal of Applied Physics **12**(8) (1973) 1130-1138.
[22] G.P. Sorokin and A.P. Paradenko, Izvestiya Vuzov. Fizika (USSR) **5** (1966) 91-95. (in Russian)